Tidal Resource Gaps Analysis Technical Report

Levi Kilcher,[1] Kevin Haas,[2] and Alexandra Muscalus[2]

1 National Renewable Energy Laboratory
2 Georgia Institute of Technology

NREL is a national laboratory of the U.S. Department of Energy
Office of Energy Efficiency & Renewable Energy
Operated by the Alliance for Sustainable Energy, LLC

This report is available at no cost from the National Renewable Energy Laboratory (NREL) at www.nrel.gov/publications.

Contract No. DE-AC36-08GO28308

Technical Report
NREL/TP-5700-86692
September 2023

Tidal Resource Gaps Analysis Technical Report

Levi Kilcher,[1] Kevin Haas,[2] and Alexandra Muscalus[2]

1 National Renewable Energy Laboratory
2 Georgia Institute of Technology

Suggested Citation
Kilcher, Levi, Kevin Haas, and Alexandra Muscalus. 2023. *Tidal Resource Gaps Analysis Technical Report*. Golden, CO: National Renewable Energy Laboratory. NREL/TP-5700-86692. https://www.nrel.gov/docs/fy23osti/86692.pdf.

NREL is a national laboratory of the U.S. Department of Energy
Office of Energy Efficiency & Renewable Energy
Operated by the Alliance for Sustainable Energy, LLC

This report is available at no cost from the National Renewable Energy Laboratory (NREL) at www.nrel.gov/publications.

Contract No. DE-AC36-08GO28308

Technical Report
NREL/TP-5700-86692
September 2023

National Renewable Energy Laboratory
15013 Denver West Parkway
Golden, CO 80401
303-275-3000 • www.nrel.gov

NOTICE

This work was authored in part by the National Renewable Energy Laboratory, operated by Alliance for Sustainable Energy, LLC, for the U.S. Department of Energy (DOE) under Contract No. DE-AC36-08GO28308. Funding provided by U.S. Department of Energy Office of Energy Efficiency and Renewable Energy Water Power Technologies Office. The views expressed herein do not necessarily represent the views of the DOE or the U.S. Government.

This report is available at no cost from the National Renewable Energy Laboratory (NREL) at www.nrel.gov/publications.

U.S. Department of Energy (DOE) reports produced after 1991 and a growing number of pre-1991 documents are available free via www.OSTI.gov.

Cover Photos by Dennis Schroeder: (clockwise, left to right) NREL 51934, NREL 45897, NREL 42160, NREL 45891, NREL 48097, NREL 46526.

NREL prints on paper that contains recycled content.

Acknowledgments

Thanks to the U.S. Department of Energy's Water Power Technologies Office for funding for this Tidal Gaps Analysis project.

List of Acronyms

DOE	U.S. Department of Energy
GC05	Garrett and Cummins, 2005
IEC	International Electrotechnical Commission
LIS	Long Island Sound
NREL	National Renewable Energy Laboratory
PNNL	Pacific Northwest National Laboratory
RA	Resource Assessment, “Assessment of Energy Production Potential from Tidal Streams in The United States” (Haas et al. 2011)
TPD	tidal power density

Executive Summary

The tidal resource gaps project was created to address a growing body of evidence that models underpredict tidal current speeds compared to measurements at a number of the top-ranking tidal energy sites. This led to industry and U.S. Department of Energy concerns that the U.S. tidal energy resource assessment (RA), which is based primarily on models, may be an underestimate.

In response, this project compared opportunistic tidal power density (TPD) measurements from 16 tidal energy "Hot Spot" sites with estimates from RA data to identify discrepancies. Comparisons were made at the location of the measurements and not necessarily the location reported in the RA or the location with the highest energy density. The sites most underestimated in the RA model data were East River, New York (−87%); Long Island Sound, New York (−51%); and Craig, Alaska (−45%). The sites most overestimated by the RA are Seven Mile Bridge, Florida (+1129%), Rich Passage, Washington (+418%); Dana Passage, Washington (+284%); Key West, Florida (+244%); Quicks Hole, Massachusetts (+176%); Tacoma Narrows, Washington (+134%); Portsmouth Harbor, Maine/New Hampshire (+53%), and Cook Inlet, Alaska (+35%).

To improve the accuracy of resource estimates from model data, updated data from eight improved model simulations were obtained. The Long Island Sound model was updated for this project, and additional model updates—namely, Cook Inlet, Alaska; Delaware Bay, Delaware; Florida Keys, Florida; Maine; Massachusetts, Portsmouth Harbor, New Hampshire; and Salish Sea, Washington—were obtained from separate projects. Model improvements included grid refinement, domain coupling, and the use of unstructured or nested grids. New TPD resource estimates were calculated from the updated models and used to rank the sites for an update to the Hot Spots list.

Improvements were also made to the method of determining the total theoretical resource of a site, which directly influences the "market" factor in the Hot Spots ranking. The method, from Garrett and Cummins (2005), uses model data to estimate the theoretical resource available to a full fence of turbines spanning a channel. Assumptions underlying the method derivation, such as uniform flow, are not always met at RA sites, but the efficiency of the method was critical for its implementation on a national scale in the RA. In this project, modifications to the application of the method were made in order to better represent nonuniform flow, resulting in more accurate channel flow rates and reduced spatial sensitivity of the resource estimate. For a given site, these modifications may either increase or decrease the total resource. Efforts to identify a pathway for quantifying changes to the total resource is within the scope of the ongoing Resource Characterization project.

The Hot Spots list was updated with TPD estimates from the improved models and the market factor from the improved theoretical resource calculation method. Significant changes include the increase in rank of the East River, New York, site from Rank 30 to Rank 3. Similarly, the Long Island Sound Entrance site increased from Rank 11 to Rank 4. Cape Cod was added to the ranking list because of the availability of new data, and it is now at Rank 13. Delaware Bay, which previously fell below the ranking threshold due to insufficient energy density, now has a higher energy density and is ranked at Rank 20.

Table of Contents

List of Figures

List of Tables

1 Introduction

1.1 Background

The U.S. Department of Energy (DOE)-funded resource assessment, "Assessment of Energy Production Potential from Tidal Streams in The United States" (Haas et al. 2011), hereafter referred to as the Resource Assessment or RA, is the most comprehensive estimate of the U.S. tidal energy resource. Produced by applying the Garrett and Cummins (2005), or GC05, method of calculating the maximum theoretical tidal energy resource (i.e., theoretical resource) to the tidal constituent output of numerical model simulations for over 200 sites, it has provided the tidal energy industry and DOE with a baseline for evaluating tidal energy market potential and siting opportunities.

Additionally, siting opportunities for tidal energy projects have been prioritized with a list of tidal energy "Hot Spots" in the DOE-funded report *Marine Hydrokinetic Energy Site Identification and Ranking Methodology Part II: Tidal Energy* (Kilcher and Thresher 2016). This report presents a methodology for identifying and ranking sites using not only tidal energy density but also the following site characteristics important to project development: market size, range between the resource and the nearest power grid transmission point, water depth, shipping cost for building and maintaining a tidal energy facility, and regional energy price. The report analysis identified and ranked 36 U.S. sites meeting viability criteria for the aforementioned characteristics, such as total power densities exceeding 0.5 kW/m^2 and distances to transmission not exceeding 20 km.

1.2 Motivation

The tidal resource gaps project was created to address a growing body of evidence that models underpredict tidal current speeds compared to measurements at a number of the top-ranking tidal energy sites. This led to industry and DOE concerns that the U.S. tidal energy RA, which is based primarily on models, may be an underestimate. In addition, questions have arisen regarding the applicability of the GC05 resource calculation method, particularly regarding the idealized channel assumptions for which the method was derived. Many locations where the RA applied that method do not match the idealized conditions, particularly the assumption of uniform flow across a channel cross section. The goal of this project, therefore, is to perform a systematic review of the tidal energy RA methodology—including a detailed investigation of the model validation data sets and procedures, as well as the application of the GC05 theoretical resource calculation method—and to propose changes or update results where possible.

Furthermore, as part of the dissemination strategy for the "Model Validation and Site Characterization for Early Deployment MHK Sites and Establishment of Wave Classification Scheme" project (hereafter, "Resource Characterization project") NREL has been communicating with the Marine Energy Council's resource assessment subcommittee. Those conversations have pointed out that the uncertainties in the tidal energy resource estimates complicate the task of identifying early market tidal energy sites. To address these concerns, this project quantifies discrepancies between modeled and measured tidal energy power density at sites that are identified in Kilcher and Thresher (2016), and that already have publicly available measurements. This will provide DOE and the tidal energy industry with a clearer understanding of the accuracy of the existing tidal energy RA.

1.3 Objectives

The objectives of this project were:

1. Estimate the uncertainty in the existing estimates of theoretical tidal power density resource estimates
2. Determine the sources of discrepancy in the national tidal energy RA
3. Develop plans for addressing the discrepancies; improve the Long Island Sound (LIS) model for comparison with extensive energy density measurements
4. Modify the application method of GC05 to better account for nonuniform flow and lessen spatial sensitivity
5. Revise the rankings of the Hot Spots using improved model data, including new data from the "Model Validation and Site Characterization for Early Deployment MHK Sites and Establishment of Wave Classification Scheme" project by the Pacific Northwest National Laboratory (PNNL).

1.4 Project Overview

First, tidal energy density measurements of the Hot Spot sites were compared to resource estimates in the RA to identify discrepancies. Where possible, model improvements were implemented to provide more accurate modeling of the tidal velocities and recalculate the resource. In addition, the theoretical resource calculation method was modified to better represent nonuniform flow and reduce spatial sensitivity; this was accomplished with fine-scale constituent interpolation and accounting for the cross-channel variability of tidal constituent phases. Finally, the ranking of the Hot Spots was updated to incorporate changes in power density resulting from updated model data.

2 Tidal Power Density Discrepancy Identification

Velocity and water level data were obtained from the cmist.noaa.gov website for locations near the Hot Spots sites; data were available for a total of 16 sites. In addition, a recent journal paper provided measurement data for the East River, New York, site (Gunawan, Neary, and Colby 2014). The data were then analyzed according to international technical specifications (IEC 2015) to estimate tidal power density (TPD), tidal amplitude, and tidal velocity.

For each measurement site, the TPD was also computed from the RA model data. The percent difference between the measured TPD and that based on RA data was used to identify discrepancies in the TPD. These values are presented in Table 1, with positive percent difference indicating that the RA data overpredicted the power density, and a negative percent difference indicating that the RA data underpredicted the power density.

The sites most underestimated in the RA data are East River, New York (−87%); Long Island Sound, New York (−51%); and Craig, Alaska (−45%).

The sites most overestimated by the RA are Seven Mile Bridge, Florida (+1129%), Rich Passage, Washington (+418%); Dana Passage, Washington (+284%); Key West, Florida (+244%); Quicks Hole, Massachusetts (+176%); Tacoma Narrows, Washington (+134%); Portsmouth Harbor, Maine/New Hampshire (+53%), and Cook Inlet, Alaska (+35%).

The sites with agreement within 20% are Western Passage, Maine (−18%); Kodiak, Alaska (+12%); San Francisco Bay, California (+3%); and St. Mary’s River, Georgia/Florida (0%).

Because measurements were opportunistic, comparisons were not necessarily made at the location of the most intense resource or the precise location reported for the site in the RA. Promising high-priority sites with large discrepancies would benefit from measurements obtained in high-TPD locations to quantify the discrepancies in the more precise region of interest.

Lastly, it is important to note that because these changes reflect only changes to the local TPD, they do not represent changes to the total theoretical resource. Further work to identify a pathway for quantifying changes to the total resource is within the scope of the ongoing Resource Characterization project.

Table 1. Discrepancies Between the RA and Measured Energy Densities

Site	State	Measured Power Density (W/m2)	RA Power Density (W/m2)	RA vs. Measured Power Density (% Difference)	Measurement Source
Western Passage	ME	364	297	−18	CMIST: EPT0003
Tacoma Narrows	WA	1,991	4,669	134	CMIST: PUG1527
Cook Inlet	AK	3,956	5,344	35	CMIST: COI0503
Portsmouth Harbor	ME,NH	911	1,397	53	CMIST: PIR0705
Kodiak	AK	2,080	2,328	12	CMIST: KOD0931
San Francisco Bay	CA	424	436	3	CMIST: SFB1203
Long Island Sound	NY	1,007	494	−51	CMIST: LIS1001
Dana Passage	WA	277	1,065	284	CMIST: PUG1539
St. Mary's River	GA,FL	563	563	0	CMIST: FEB1102
Rich Passage	WA	518	2,683	418	CMIST: PUG1514
Woods Hole Passage	MA	100	510	411	CMIST: COD0912
Key West	FL	139	479	244	CMIST: FLK1315
Seven Mile Bridge	FL	87	1,066	1,129	CMIST: FLK1324
Quicks Hole	MA	182	502	176	CMIST: COD0914
Spanish Harbors	FL				CMIST: FLK1327
East River	NY	2,300	300	−87	Gunawan et al. 2014
Craig	AK	2,846	1,555	−45	CMIST: SEA0706

3 Numerical Model Improvements

To address accuracy issues of the model data used in the RA, updated data from eight improved model simulations were obtained. The LIS model, encompassing the East River and Long Island Sound, was updated specifically for this project. Through synergistic efforts, additional model updates were obtained from separate projects. While the LIS model data are used in Section 3.5 to demonstrate specific model improvements, all new model results were implemented in the updated Hot Spots rankings and have been updated in the Marine Energy Atlas (NREL n.d.).

3.1 Improvements by Domain

Table 2 lists the models that were improved, including the names of RA and Hot Spot sites within the domain, as well as specific model improvements and the laboratories, with the corresponding project names, that produced the new model data. Many of the updated models were run by PNNL for the Resource Characterization project. The Massachusetts sites were updated based on a new publication providing model results for that region (Cowles, Hakim, and Churchill 2017). The improvements to Georgia Tech's LIS model were produced specifically for this project, whereas Georgia Tech's Portsmouth Harbor, Delaware Bay, and Florida Keys models were updated for unrelated NREL projects supporting U.S. Department of Defense facilities.

Table 2: Overview of Model Improvements

Model Name ***RA and/or Hot Spot sites***	**Improvements**	**Laboratory** ***Project***	**Data Availability**
Cook Inlet, AK *Cook Inlet*	unstructured grid – higher resolution	PNNL *Resource Characterization (NREL)*	Atlas: No Hot Spots: No
Maine: *Western Passage* *Cobscook Bay*	unstructured grid – higher resolution	PNNL *Resource Characterization (NREL)*	Atlas: No Hot Spots: No
Salish Sea, WA: *Tacoma Narrows* *Rosario Strait* *Bellingham Channel* *San Juan Channel* *Friday Harbor* *Admiralty Inlet* *Spieden Channel* *Dana Passage* *Rich Passage* *New Channel*	unstructured grid – higher resolution	PNNL *Resource Characterization (NREL)*	Atlas: No Hot Spots: No
Massachusetts: *Vineyard Sound* *Muskeget Channel* *Nantucket Sound*	new model data available	Cowles, Hakim, and Churchill (2017)	Atlas: No Hot Spots: Yes

Model Name *RA and/or Hot Spot sites*	Improvements	Laboratory *Project*	Data Availability
Woods Hole Passage *Quicks Hole*			
Long Island Sound (LIS) *Entrance to Long Island Sound* *East River*	original domain coupled to the New York Bight; higher resolution	Georgia Tech *Tidal Gaps*	Atlas: Yes Hot Spots: Yes
Portsmouth Harbor, ME/NH *Portsmouth Harbor*	nested grid – higher resolution	Georgia Tech *Navy Tidal Modeling: Resource Maps and Data (NREL)*	Atlas: Yes Hot Spots: Yes
Delaware Bay, DE *Delaware Bay*	nested grids – higher resolution; new data available	Georgia Tech *Navy Base Tidal Stream Energy Resource Assessment (NREL)*	Atlas: Yes Hot Spots: Yes
Florida Keys, FL *Key West* *Seven Mile Bridge*	nested grid – higher resolution	Georgia Tech *Navy Base Tidal Stream Energy Resource Assessment (NREL)*	Atlas: Yes. Hot Spots: Yes

3.2 Example: Long Island Sound, New York

The improved model simulation for LIS is documented here as an illustration of the model improvements addressing the resource assessment shortcomings. The most significant change is coupling the two model domains of LIS with the New York Bight via the East River. The full updated, coupled model domain is compared to the original separate domains in Figure 1. In addition to the grid coupling, the model resolution is increased in the vicinity of Roosevelt Island in the East River. The resolution and power density of the original and improved models, within the vicinity of Roosevelt Island, are compared in Figure 2.

Table 3 provides the tidal velocity constituents for the old and new models and demonstrates significant reduction in the discrepancy between model and observations for the tidal velocity amplitudes. For example, the dominant M2 constituent amplitude difference is decreased from −1.148 m/s to −0.044 m/s, and the difference in the second-largest amplitude constituent, S2, decreases from −0.237 m/s to 0.005 m/s.

The power density in the East River in the improved model is in much better agreement with Acoustic Doppler Current Profiler observations of 2.0 kW/m^2. Whereas the old model produced an energy density of 0.5 kW/m^2, the energy density in the new model is 1.8 kW/m^2, which—while still an underestimate by 10%—is a dramatic improvement from the 75% underestimate.

Table 3: Constituents and Differences from Observations for Old and New LIS Models

Con	Amplitude (m/s)					Inclination (deg)			Phase (deg)			
	Obs	*Old Model*	*Old Diff*	New Model	New Diff	Obs.	New Mod	New Diff	Obs.	New Mod	New Diff (deg)	New Diff (min)
M2	1.982	*0.834*	*−1.148*	1.938	−0.044	61.3	58.5	−2.8	341.2	330.0	−10.3	−21.3
N2	0.291	*0.134*	*−0.157*	0.281	−0.010	60.8	58.5	−2.3	330.8	317.8	−13.0	−27.3
S2	0.307	*0.069*	*−0.237*	0.311	0.005	61.2	58.5	−2.7	14.5	1.7	−12.7	−25.5
K1	0.026	*0.014*	*−0.012*	0.049	0.023	63.3	58.9	−4.5	94.7	77.4	−17.3	−69.2
O1	0.054	*0.018*	*−0.036*	0.051	−0.002	61.1	59.0	−2.2	111.6	102.6	−9.0	−38.6
M4	0.097	*0.017*	*−0.081*	0.046	−0.050	64.4	53.3	−11.1	335.6	329.0	−6.6	−6.9

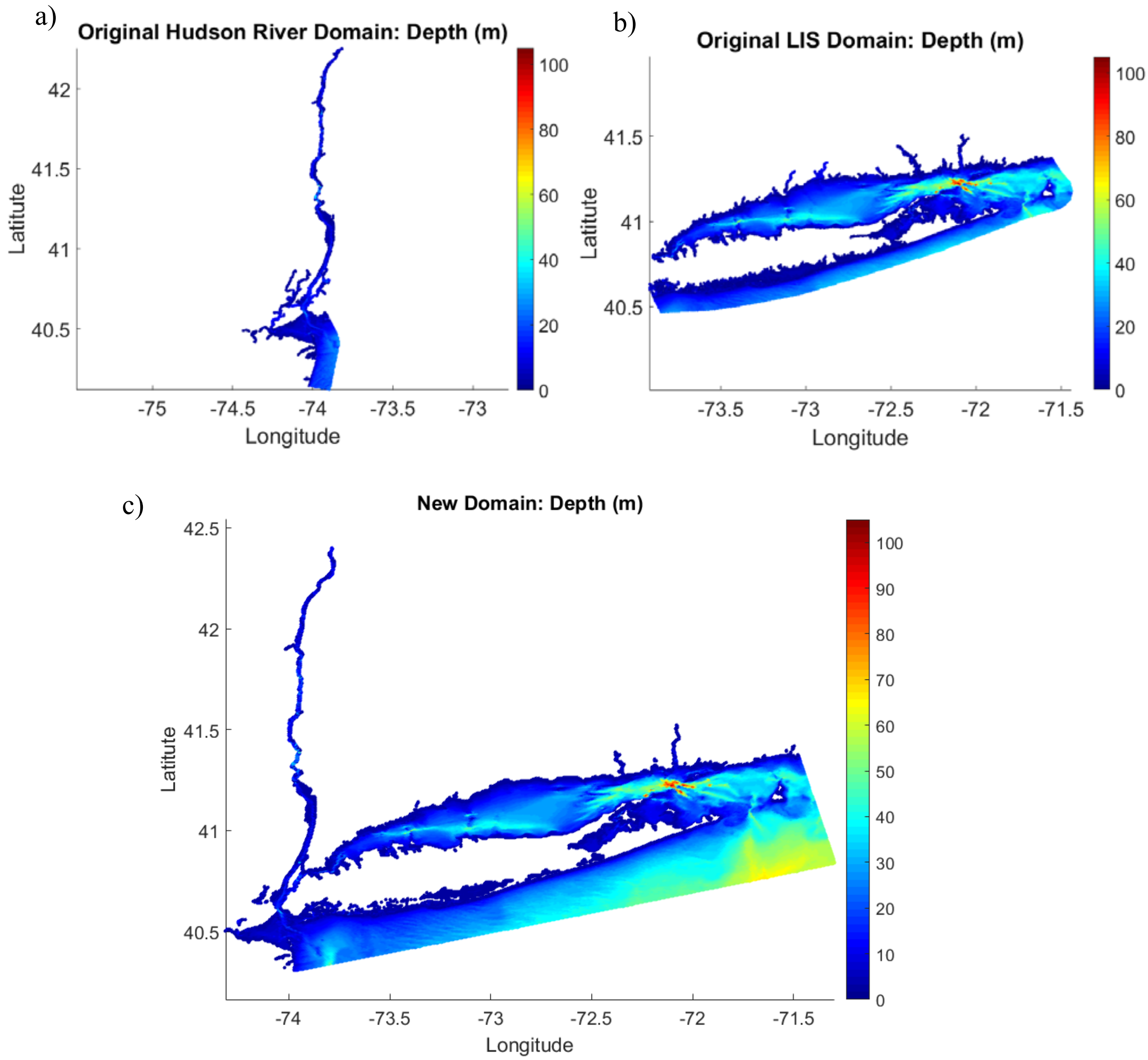

Figure 1: The original domain was separated into (a) the Hudson River and (b) the Long Island Sound (LIS), whereas the new domain (c) couples those two regions.

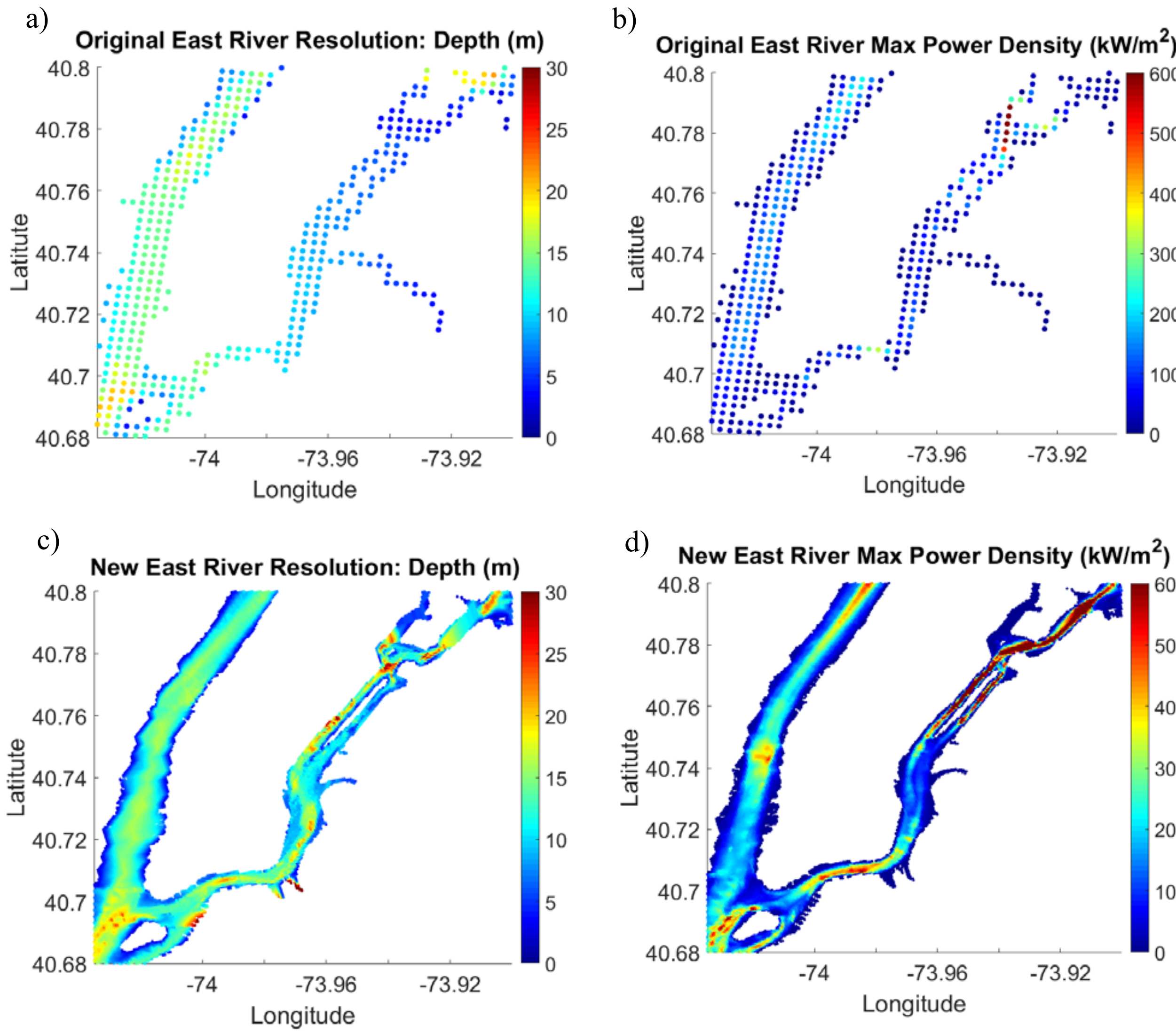

Figure 2: The original model resolution of the East River (a) bathymetry and (b) maximum power density was coarse, whereas the new model (c) bathymetry and (d) maximum power are significantly improved and have higher maximum power values.

4 Improvements to the Theoretical Resource Calculation Method

The “market” attribute of a site, provided on the Hot Spots list and utilized in site ranking, is dependent on the theoretical resource of the site. This resource is efficiently estimated with the GC05 method, which assumes a full fence of tidal turbines spanning an idealized channel with uniform flow. The benefit of this method is that it may be applied to many sites on a large scale, using numerical model data without accounting directly for the effect of energy extraction within the model. However, the conditions for which it was derived are not met at many of the RA sites. In other words, the RA assumes that the GC05 method is more accurate than alternatives based on weaker assumptions, but it still leaves significant room for improvement. It has become particularly apparent that in many cases the method, as applied in the original RA, is unrealistically sensitive to the precise transect location. To address this, we proposed two improvements to the application of the method: (1) We increased the accuracy of mapping constituents onto the theoretical transect and (2) we decreased the spatial sensitivity of the resource estimate to the precise transect location by accounting for phase variation across a channel.

4.1 Fine-Scale Interpolation

In the original RA, constituent data are mapped onto a transect, representing a theoretical full fence of turbines, at the model grid resolution. This leaves the end regions of the transect particularly susceptible to mapping errors, which may in turn introduce errors into the total flow across the transect and therefore the theoretical resource estimate at the transect.

To avoid this, a fine-scale linear interpolation, at approximately 10 times the grid resolution, has replaced the grid-scale mapping. This produces more realistic variation in fluxes along the length of the transect and is particularly adept at representing flow near the transect end points.

4.2 Discrete Phase

In the RA, the constituent phase was assumed constant along the transect, but the inclination angle varied spatially at the grid resolution. This produced instances when the inclination angle of a particular constituent on a transect segment might be reversed by 180 degrees from the inclination angle of the neighboring segment; realistically, the inclination angle reversal is accompanied by a significant phase shift, together resulting in essentially unidirectional flow. However, when the phase is assumed constant for the full transect, the phase cannot be shifted in the region with the reversed inclination, producing a false region of “reverse flow.” In the improved method, both inclination angle and constituent phase are allowed to vary at the fine-scale resolution of the interpolation, preventing the erroneous flow reversals.

4.3 Example: San Francisco Bay, California

San Francisco Bay exhibits regions of erroneous flow reversal using the original application method of GC05; this is shown in Figure 3 (upper). The region east of the labeled headland appears to have a weak reverse flow with respect to the center channel flow. However, this is due to a flip in inclination angle that in reality is accompanied by a phase shift; this phase shift is not captured in the original method, so the region appears to have a negative flow, which serves to decrease total flow and thus the maximum theoretical power across the transect.

When phase is allowed to vary discretely across the transect, as in Figure 3 (lower), the region east of the headland exhibits a weak flow in the same direction as that in the center of the channel. For transects affected by the phase shift, the total flow across the transect has the potential to increase, and therefore the theoretical maximum power across affected transects may increase as well.

It is important to note that in addition to correcting flow reversal due to the combination of inclination flips and phase shifts, the incorporation of a spatially varying phase commonly serves to decrease the total flow across transects. This is because all segments are no longer assumed to be in phase with each other, and thus the maximum total flow across the transect does not necessarily capture all the maximum flow rates of all the discrete segments. Rather, a time series of the flow rate summed across all discrete segments is produced, and the maximum flow rate used in the maximum power calculation is taken as the maximum of that time series. This concept is illustrated in Figure 4.

In the San Francisco case, both of these effects of incorporating a spatially varying phase are demonstrated in the theoretical maximum power of each transect, which is highly reflective of the maximum flow rate. Figure 5 compares the maximum power of each transect as calculated with a constant phase at each transect (upper plot) and a spatially varying phase at each transect (lower plot). The use of the spatially varying phase improves the uniformity of the power throughout the bay entrance and slightly decreases the power in transects unaffected by flow reversals. In transects exhibiting flow reversals in Figure 3 (upper), the total power increases due to the correction of the reversals. Thus, the new method of applying GC05 may either increase or decrease the power of a given transect. Regardless of whether a particular transect increases or decreases, the spatial sensitivity of the calculation to a particular transect is reduced, and we believe that this increased consistency reduces uncertainty in the GC05 calculations, which results in an improvement to the theoretical resource estimation.

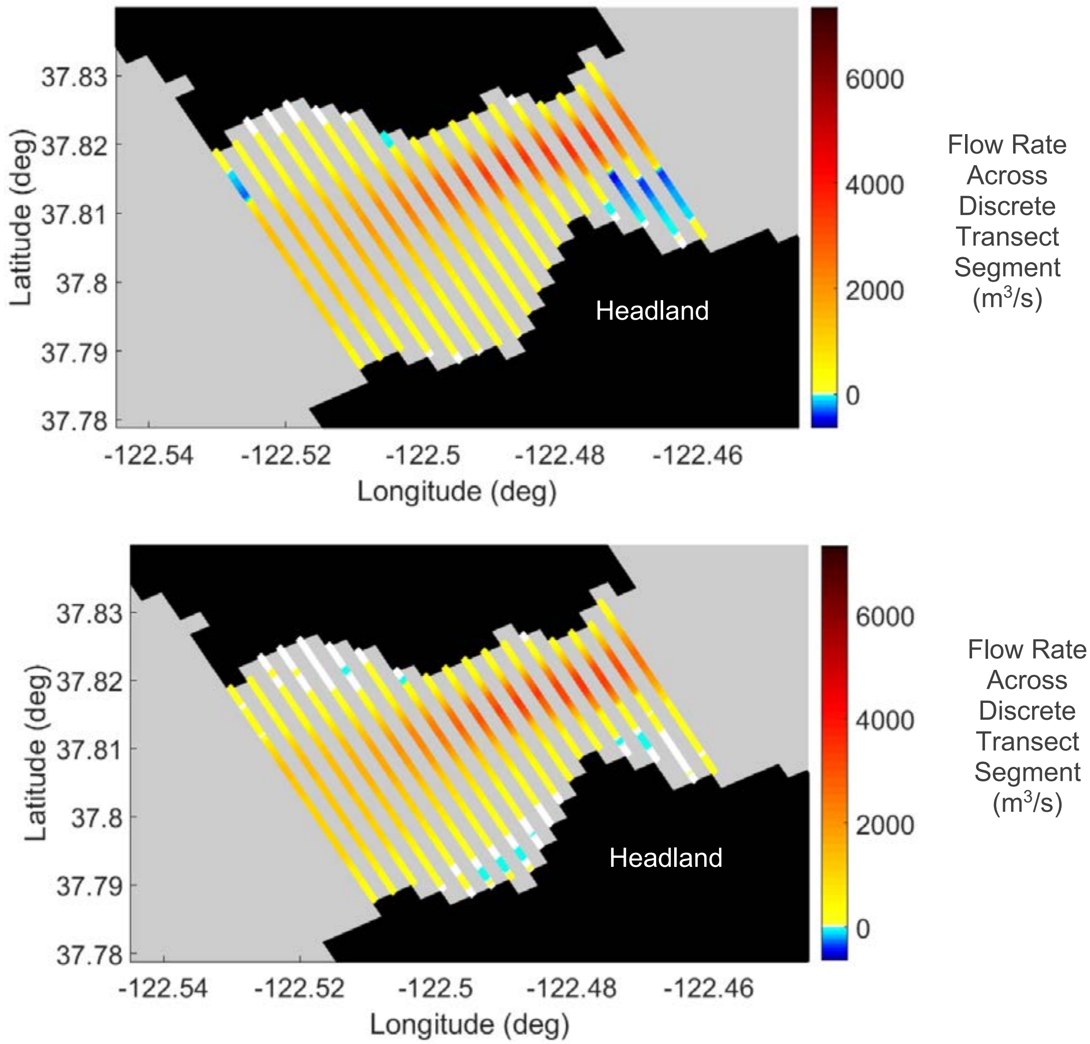

Figure 3: Flow across each segment of multiple transects at the entrance to San Francisco Bay, comparing the (Upper) presence of reversed flow regions produced by using a constant phase for each transect to (Lower) the absence of reversed flow regions when phase variation along a transect is accounted for in the flow calculation

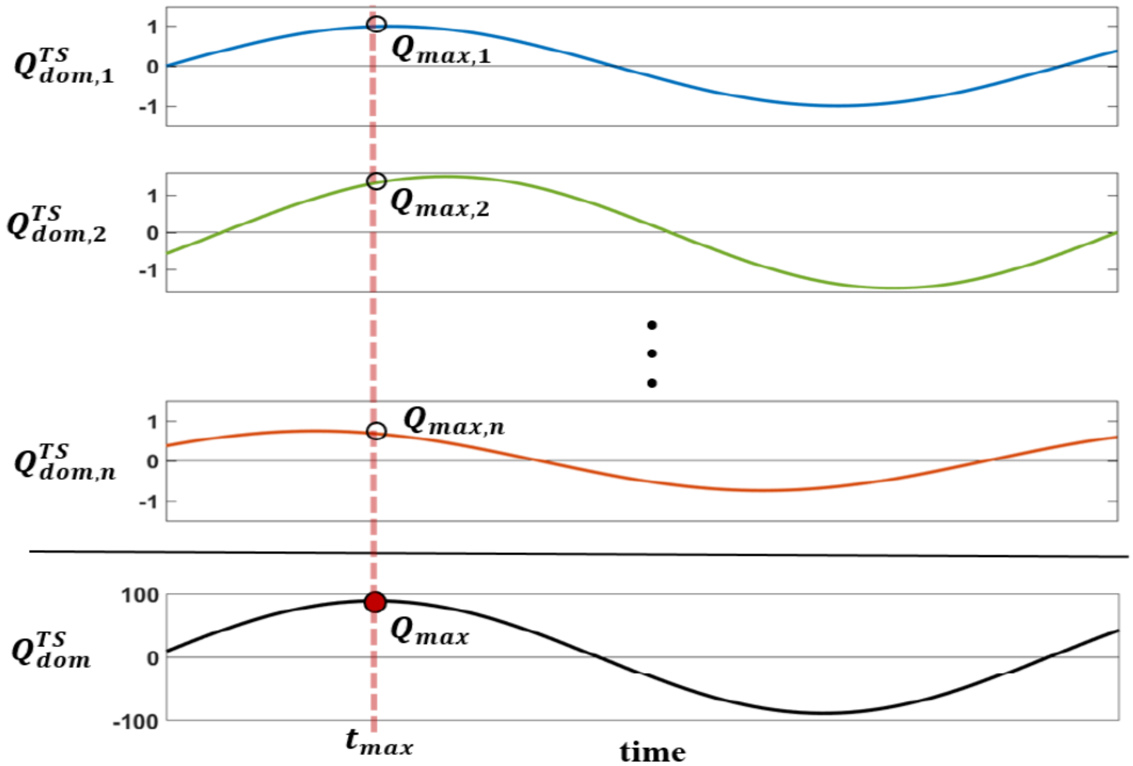

Figure 4: Illustration of the calculation method for maximum total flow rate, Q_{max}, across a transect with spatially varying phase. Due to the variation of phase, discrete transect segment flow rates, may not be at their maximum flow value at the time t_{max} corresponding to Q_{max}.

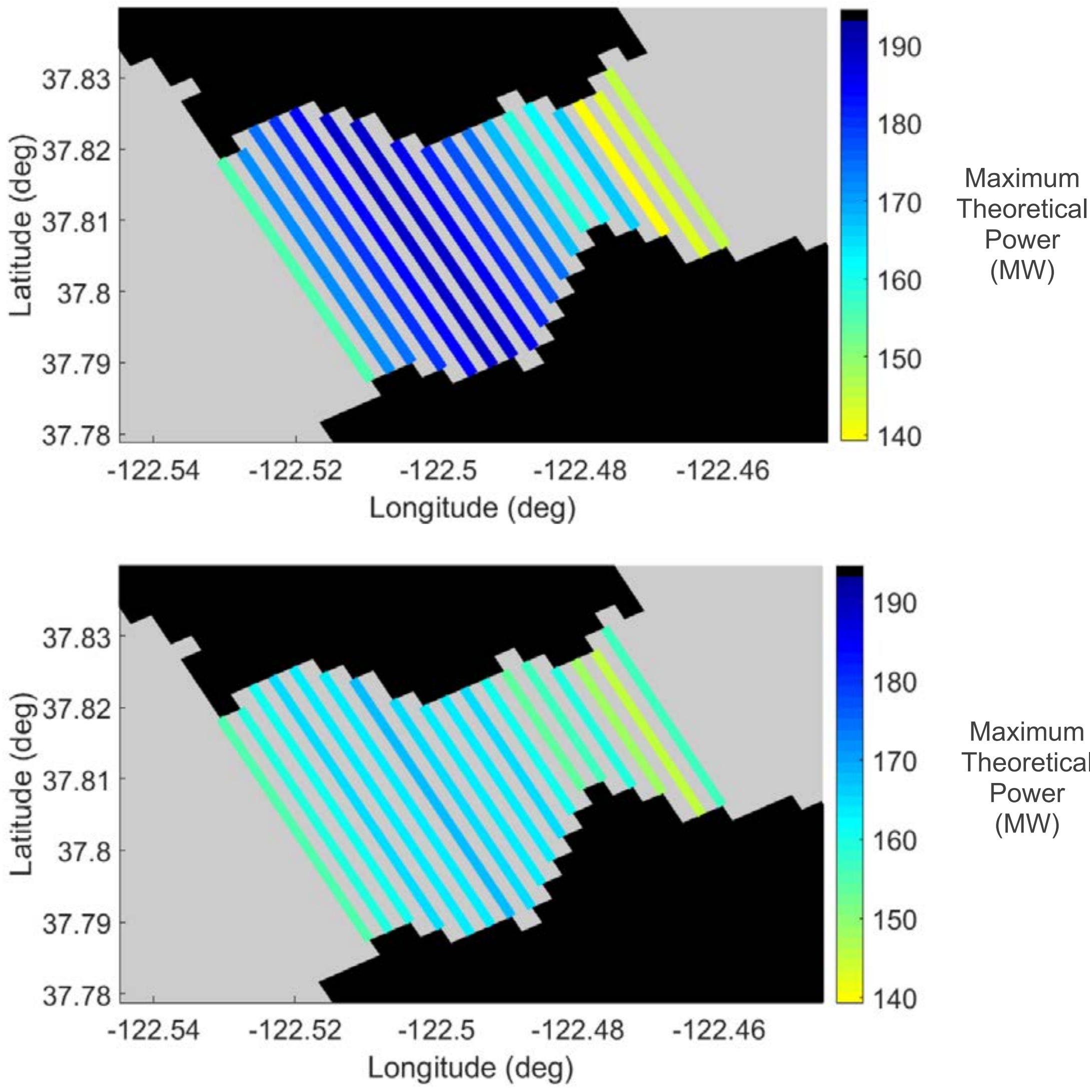

Figure 5: Maximum theoretical power (MW) of multiple transects at the entrance to San Francisco Bay comparing the spatial variation in power calculated with (Upper) a constant phase for each transect and (Lower) a spatially varying phase across the discrete segments of each transect

5 Hot Spots Updates

Using the new model results for power density calculations, the Hot Spots ranking lists are updated for the 'short term' model (table 4) and long-term model (table 5). Descriptions of scoring categories and ranking methodology are provided in Kilcher et al. (2016). Yellow indicates sites with updated data, and darker greens indicate higher scores in each category. "L" and "R" in the market column indicate whether the site is primarily loaded or resource limited. Each scoring criterion is weighted equally (1/5 in the long-term model and 1/6 in the short-term model) to compute the total score. The right column includes the rank change (blue: up, red: down) relative to the previous ranking in Kilcher et al. (2016).

Noteworthy changes to the rankings due to the new model data described here include:

- The East River, New York, increased from Rank 30 to Rank 3.
- The Long Island Sound Entrance site increases from Rank 11 to Rank 4.
- Very little changes in energy density resulted from the improved modeling of Portsmouth Harbor, and this site decreased from Rank 8 to Rank 9 due only to the increased energy density of other sites.
- Cape Cod was added to the ranking list because of the availability of new data, and it is now at Rank 13.
- Delaware Bay, which previously fell below the ranking threshold due to insufficient energy density, now has a higher energy density and is ranked at Rank 20.

Table 4: Short-Term Hot Spots Ranking

	Site	State	Lat	Lon	Resource [kW/m^2]	Market [MW]	Range [km]	Shipping [$/ton]	Depth [m]	Score	Rank Change
1	Tacoma Narrows	WA	47.28	-122.55	2.0	210 R	1.4	0	33	9.9	0
2	Western Passage	ME	44.92	-66.99	3.0	190 R	1.1	0	35	9.8	0
3	Rosario Strait	WA	48.58	-122.75	2.2	420 R	3.5	0	50	9.7	0
4	Cook Inlet	AK	60.79	-151.26	2.1	500 L	2.5	91	41	9.7	0
5	Bellingham Channel	WA	48.56	-122.67	2.0	130 R	4.0	0	24	9.4	0
6	San Juan Channel	WA	48.46	-122.95	2.0	160 R	7.0	0	56	9.1	0
7	East River	NY	40.79	-73.92	2.1	16 R	0.3	0	21	8.9	26
8	Vineyard Sound	MA	41.48	-70.64	1.7	84 R	5.1	0	23	8.8	-1
9	Muskeget Channel	MA	41.35	-70.37	2.4	90 R	8.3	0	23	8.7	-1
10	Long Island Sound	NY	41.23	-72.07	1.2	250 R	4.2	0	20	8.6	4
11	Portsmouth Harbor	ME,NH	43.07	-70.73	2.6	16 R	3.9	0	20	8.6	-2
12	Friday Harbor	WA	48.54	-122.98	1.0	180 R	3.5	0	48	8.3	-2
13	Admiralty Inlet	WA	48.14	-122.70	0.9	720 R	6.6	0	48	7.9	-2
14	Cape Cod Canal	MA	41.74	-70.61	1.5	5.0 R	1.6	0	20	7.8	NEW
15	Kodiak	AK	57.79	-152.41	3.6	16 L	9.3	114	27	7.8	-3
16	San Francisco Bay	CA	37.82	-122.48	0.7	170 R	4.8	0	32	7.7	-3
17	Spieden Channel	WA	48.63	-123.12	1.4	160 R	12.7	0	30	7.5	-2
18	Dana Passage	WA	47.17	-122.86	1.9	47 R	10.6	0	13	7.2	-2
19	St. Mary's River	GA,FL	30.71	-81.45	0.8	13 R	3.1	0	18	7.0	-2
20	Columbia River	OR,WA	46.25	-124.02	1.8	81 R	13.0	0	14	6.9	-2
21	Rich Passage	WA	47.59	-122.56	2.0	16 R	3.8	0	10	6.8	-2
22	Nantucket Sound	MA	41.51	-69.97	2.0	260 R	17.4	0	20	6.6	-2
23	Delaware Bay	NJ,DE	38.86	-75.03	0.9	320 R	6.6	0	11	6.5	15*
24	Cobscook Falls	ME	44.88	-67.13	1.1	13 R	7.3	0	11	5.9	-3
25	Coos Bay	OR	43.35	-124.34	1.4	9.1 R	3.0	0	8	5.8	-3
26	New Channel	WA	48.66	-123.14	0.8	100 R	16.4	0	33	5.7	-3
27	Woods Hole Passage	MA	41.52	-70.68	0.6	3.1 R	7.2	0	18	5.7	-3
28	Hatteras Inlet	NC	35.19	-75.76	1.4	6.2 R	5.8	0	9	5.6	-3
29	Key West	FL	24.56	-81.83	0.8	14 R	2.4	0	9	5.5	-3
30	Seven Mile Bridge	FL	24.70	-81.15	0.9	27 R	4.5	0	8	5.4	-3
31	Guemes Channel	WA	48.52	-122.62	1.4	16 R	1.5	0	7	5.4	-3
32	Quicks Hole	MA	41.44	-70.84	1.2	11 R	15.9	0	14	5.2	-3
33	Dillingham	AK	59.04	-158.46	1.4	2.1 L	6.6	250	12	5.2	-3
34	Spanish Harbors	FL	24.65	-81.29	0.7	7.9 R	6.1	0	9	5.0	-3
35	Turtle River	GA	30.98	-81.52	0.5	10 R	4.8	0	8	4.7	-3
36	Ocracoke Inlet	NC	35.07	-76.02	0.7	7.5 R	11.4	0	8	4.3	-2
37	Craig	AK	55.48	-133.15	1.7	1.3 L	19.0	71	14	3.5	-2
38	Charlotte Harbor	FL	26.71	-82.26	1.0	8.8 R	19.6	0	13	3.0	-2

Table 5: Long-Term Hot Spots Ranking

	Site	State	Lat	Lon	Resource [kW/m^2]	Market [MW]	Energy Cost [$/kWh]	Range [km]	Shipping [$/ton]	Depth [m]	Score	Rank Change
1	Cook Inlet	AK	60.79	-151.26	2.1	500 L	0.16	2.5	91	41	8.0	0
2	Western Passage	ME	44.92	-66.99	3.0	190 R	0.14	1.1	0	35	8.0	0
3	East River	NY	40.79	-73.92	2.1	16 R	0.19	0.3	0	21	7.7	27
4	Long Island Sound	NY	41.23	-72.07	1.2	250 R	0.19	4.2	0	20	7.5	7
5	Vineyard Sound	MA	41.48	-70.64	1.7	84 R	0.16	5.1	0	23	7.4	-2
6	Muskeget Channel	MA	41.35	-70.37	2.4	90 R	0.16	8.3	0	23	7.4	-2
7	Tacoma Narrows	WA	47.28	-122.55	2.0	210 R	0.09	1.4	0	33	7.4	-2
8	Rosario Strait	WA	48.58	-122.75	2.2	420 R	0.09	3.5	0	50	7.3	-2
9	Portsmouth Harbor	ME,NH	43.07	-70.73	2.6	16 R	0.15	3.9	0	20	7.2	-1
10	Bellingham Channel	WA	48.56	-122.67	2.0	130 R	0.09	4.0	0	24	7.1	-3
11	San Juan Channel	WA	48.46	-122.95	2.0	160 R	0.09	7.0	0	56	6.9	-2
12	Kodiak	AK	57.79	-152.41	3.6	16 L	0.18	9.3	114	27	6.8	-2
13	Cape Cod Canal	MA	41.74	-70.61	1.5	5.0 R	0.16	1.6	0	20	6.7	NEW
14	San Francisco Bay	CA	37.82	-122.48	0.7	170 R	0.16	4.8	0	32	6.7	-2
15	Friday Harbor	WA	48.54	-122.98	1.0	180 R	0.09	3.5	0	48	6.4	-2
16	Admiralty Inlet	WA	48.14	-122.70	0.9	720 R	0.09	6.6	0	48	6.2	-2
17	Spieden Channel	WA	48.63	-123.12	1.4	160 R	0.09	12.7	0	30	5.9	-2
18	Nantucket Sound	MA	41.51	-69.97	2.0	260 R	0.16	17.4	0	20	5.9	-2
19	St. Mary's River	GA,FL	30.71	-81.45	0.8	13 R	0.11	3.1	0	18	5.8	-2
20	Delaware Bay	NJ,DE	38.86	-75.03	0.9	320 R	0.14	6.6	0	11	5.7	18*
21	Dana Passage	WA	47.17	-122.86	1.9	47 R	0.09	10.6	0	13	5.7	-3
22	Columbia River	OR,WA	46.25	-124.02	1.8	81 R	0.09	13.0	0	14	5.6	-3
23	Rich Passage	WA	47.59	-122.56	2.0	16 R	0.09	3.8	0	10	5.4	-3
24	Cobscook Falls	ME	44.88	-67.13	1.1	13 R	0.14	7.3	0	11	5.3	-3
25	Dillingham	AK	59.04	-158.46	1.4	2.1 L	0.27	6.6	250	12	5.2	-3
26	Woods Hole Passage	MA	41.52	-70.68	0.6	3.1 R	0.16	7.2	0	18	5.2	-3
27	Coos Bay	OR	43.35	-124.34	1.4	9.1 R	0.10	3.0	0	8	4.8	-3
28	Quicks Hole	MA	41.44	-70.84	1.2	11 R	0.16	15.9	0	14	4.8	-3
29	Hatteras Inlet	NC	35.19	-75.76	1.4	6.2 R	0.11	5.8	0	9	4.8	-3
30	Key West	FL	24.56	-81.83	0.8	14 R	0.11	2.4	0	9	4.7	-3
31	New Channel	WA	48.66	-123.14	0.8	100 R	0.09	16.4	0	33	4.7	-3
32	Seven Mile Bridge	FL	24.70	-81.15	0.9	27 R	0.11	4.5	0	8	4.7	-3
33	Guemes Channel	WA	48.52	-122.62	1.4	16 R	0.09	1.5	0	7	4.4	-2
34	Spanish Harbors	FL	24.65	-81.29	0.7	7.9 R	0.11	6.1	0	9	4.4	-2
35	Turtle River	GA	30.98	-81.52	0.5	10 R	0.11	4.8	0	8	4.2	-2
36	Ocracoke Inlet	NC	35.07	-76.02	0.7	7.5 R	0.11	11.4	0	8	3.8	-2
37	Craig	AK	55.48	-133.15	1.7	1.3 L	0.07	19.0	71	14	3.0	-2
38	Charlotte Harbor	FL	26.71	-82.26	1.0	8.8 R	0.11	19.6	0	13	2.9	-2

6 Conclusions

Discrepancies in TPD between measurements and values calculated from RA model data have largely been addressed through improvements to portions of the model data where available. Model improvements include increased resolution, grid nesting, unstructured grids, and grid coupling. The success of these improvements indicates that updates to additional models could improve the accuracy of the resource estimates at other sites, which do not yet have updated model data. In addition, discrepancies were reported at locations of opportunistic measurements, which are not necessarily the locations reported in the RA and/or the locations with the most intense resource. Thus, measurements obtained in the locations of highest TPD at promising sites would be beneficial to the resource estimate of those sites. This project did not focus on the total national resource; efforts to identify a pathway for quantifying changes to the total resource are within the scope of the Resource Characterization project.

Improvements to the application of GC05 reduce error and spatial sensitivity resulting from the underlying assumption of uniform flow in a tidal channel. However, it remains that many RA sites violate the assumptions of the method. Additional fundamental work is needed to determine the extent to which this affects theoretical resource estimates and to investigate alternative approaches for efficiently determining the theoretical resource on a large scale.

References

Cowles, G., A. Hakim, and J. Churchill. 2017. “A Comparison of Numerical and Analytical Predictions of the Tidal Stream Power Resource of Massachusetts, USA.” Renewable Energy 114: 215–228. doi:10.1016/j.renene.2017.05.003.

Garrett, C., and P. Cummins. 2005. “The Power Potential of Tidal Currents in Channels.” Proceedings of the Royal Society A 461: 2563–2572. doi:10.1098/rspa.2005.1494.

Gunawan, B., V. S. Neary, and J. Colby. 2014. “Tidal Energy Site Resource Assessment in the East River Tidal Strait, Near Roosevelt Island, New York, NY (USA).” Renewable Energy 71: 509–517. doi:10.1016/j.renene.2014.06.002.

Haas, K. A., H. M. Fritz, S. P. French, B. T. Smith, and V. S. Neary. 2011. Assessment of Energy Production Potential From Tidal Streams in the United States. Atlanta, GA: Georgia Tech Research Institution. https://doi.org/10.2172/1219367.

International Electrotechnical Commission (IEC). 2015. Part 201: Tidal energy resource assessment and characterization (Technical Specification No. 62600–201), Marine energy - Wave, tidal and other water current converters.

Kilcher, L., and R. Thresher. 2016. Marine Hydrokinetic Energy Site Identification and Ranking Methodology Part II: Tidal Energy. Golden, CO: National Renewable Energy Laboratory. NREL/TP-5000-66079. https://dx.doi.org/10.2172/1330619.

National Renewable Energy Laboratory (NREL). No date. "Marine Energy Atlas." https://maps.nrel.gov/marine-energy-atlas.